Journal of Photonics for Energy

PhotonicsforEnergy.SPIEDigitalLibrary.org

Optimization of spray coating for the fabrication of sequentially deposited planar perovskite solar cells

Mehran Habibi
Mohammad-Reza Ahmadian-Yazdi
Morteza Eslamian

SPIE.

Mehran Habibi, Mohammad-Reza Ahmadian-Yazdi, Morteza Eslamian, "Optimization of spray coating for the fabrication of sequentially deposited planar perovskite solar cells," *J. Photon. Energy* **7**(2), 022003 (2017), doi: 10.1117/1.JPE.7.022003.

Optimization of spray coating for the fabrication of sequentially deposited planar perovskite solar cells

Mehran Habibi,[a] Mohammad-Reza Ahmadian-Yazdi,[a] and Morteza Eslamian[a,b,*]

[a]University of Michigan–Shanghai Jiao Tong University Joint Institute, Shanghai, China
[b]Shanghai Jiao Tong University, State Key Laboratory for Composite Materials, School of Materials Science and Engineering, Shanghai, China

Abstract. We use facile coating techniques including spray coating and drop casting to fabricate methylammonium lead iodide perovskite solar cells through a two-step sequential deposition approach. In the first step, for the deposition of the lead iodide, spray coating substitutes for the commonly used lab-scale spin coating, while the operating parameters of the former process are optimized to achieve a fully covered and uniform film of lead iodide. In the second step, to deposit methylammonium iodide atop the lead iodide layer to form methylammonium lead iodide perovskite, dip-coating process is replaced by the touch-free drop casting and scalable pulsed-spray coating. It is found that the performance of the perovskite films and devices made by pulsed-spray coating and drop casting is similar to those prepared by dip coating, while the large-scale production capabilities of such methods beside the low material consumptions of drop casting prove their potential to replace dip coating in large-scale manufacturing of perovskite solar cells. The champion devices fabricated by spray-drop and spin-drop techniques demonstrated power conversion efficiencies of 6.92% and 9.48%, respectively. It is expected that device fabrication in a low-humidity environment using the optimized parameters and optimization of other layers will result in higher efficiencies. [DOI: 10.1117/1.JPE.7.022003]

Keywords: perovskite solar cells; sequential deposition; drop casting; spray coating; pulsed-spray coating; optimization.

Paper 17036SS received Mar. 24, 2017; accepted for publication May 10, 2017; published online Jun. 1, 2017.

1 Introduction

Inorganic (e.g., chalcogenide), organic (e.g., polymeric), mixed inorganic-organic (e.g., perovskite), and quantum-dot thin film solar cells (SCs) are in the forefront of research and development in energy and nanotechnology fields to secure a renewable and cost-effective source of electrical energy based on the photovoltaic (PV) effect.[1,2] The aforementioned PV SCs have the potential to be fabricated using low-cost vacuum-free techniques, such as processing and casting from solutions. Organometallic perovskite SCs (PVSCs) are currently the most attractive in the abovementioned list with compelling efficiencies over 20%,[3] and therefore are the focus of this work. A recent review of the structure and advances in PVSCs is found in Ref. 2.

The perovskite light harvesting layer in a PVSC may be formed using a two-step sequential deposition strategy[4,5] or a one-step approach.[6,7] In the two-step sequential deposition, the perovskite layer, e.g., methylammonium lead iodide ($CH_3NH_3PbI_3$), is prepared in two steps. First, the PbI_2 precursor solution is deposited on the substrate by a casting method, preparing a thin layer composed of PbI_2 crystals. Then, this layer is exposed to the solution of CH_3NH_3I (MAI) to form perovskite crystals in a film. In the one-step approach, a mixture of PbI_2 and CH_3NH_3I dissolved in appropriate solvents is directly deposited on the substrate. Grätzel

*Address all correspondence to: Morteza Eslamian, E-mail: morteza.eslamian@gmail.com

et al.[4] introduced the two-step sequential deposition method as a replacement for the one-step deposition in order to achieve a better control over the perovskite film morphology. Indeed, they fabricated nearly pinhole-free perovskite films using this method. Since then, the method has been continuously improved by others using various strategies, such as vapor deposition of the two precursors[8] or well-controlled two-step spin coating.[9] Currently, the two-step sequential deposition of perovskite precursors is usually performed by spin-spin or spin-dip coating, whereas spin-coating is usually used in the one-step method. The process of film deposition may affect the film morphology, nanostructure, and optoelectronic properties, and consequently the device performance. Application of spin coating is limited to small areas in a batch process, not suitable for real-world applications.[10] Therefore, in parallel to attempts to further improve the power conversion efficiency (PCE) and stability of PVSCs, it is also essential to develop scalable techniques for future commercialization of the technology.

There are essentially a limited number of scalable techniques that can be employed to fabricate solution-processed thin films in PV and organic electronics, including spray coating, inkjet printing, slot-die coating, doctor balding or knife over edge, drop casting, gravure, and screen-printing.[5,10,11–14] Spray coating has been widely used for the fabrication of other emerging SCs, e.g., Refs. 15–20, but has not been adequately explored in the PVSC field, and only a few studies have employed it to fabricate the perovskite layer.[21–33] Due to the stochastic and random nature of droplet impact, spray-on films normally show a rough surface,[21] but the roughness can be reduced through a process optimization.[22,28] High roughness in spray-on organic SCs was reported to have negative effect on the light absorbance[10] and the device fill factor (FF),[34] although the results obtained for the organic SCs may not be necessarily applicable to crystalline perovskite SCs. By controlling the process parameters, such as substrate temperature, spray flow rate, number of spray passes, and solution concentration,[11,19,20,22,23,32,35] or applying dynamic forces on the substrate, such as ultrasonic vibration[2,5] or mechanical force (pressing),[22] the spraying process may become controllable to some extent. In some recent works, progress has been made toward fabrication of high efficiency spray-on SCs in both organic and perovskite devices.[22,36,37] Spray coating of perovskite, compared to polymeric thin films, imposes additional challenges due to the crystalline nature of perovskite and crystal formation during the process, which may cause crystallization dewetting.[13] An incomplete and dewetted perovskite layer with excessive pinholes and voids may create shunt pathways,[24] causing charge recombination and a decline in the device performance.[21]

Following the foregoing introduction and argument, in this paper, spin and dip coating, used in the sequential method, are replaced by scalable spray coating and touch-free drop casting methods. To be more specific, PbI_2 will be deposited by spray coating and the process will be optimized, then the MAI solution will be deposited atop the PbI_2 film by spray coating and also drop casting. To enhance the coverage, multiple pass spraying strategy is employed, and the effect of the number of spray passes on the film characteristics is studied. Then by controlling the solution concentration and optimizing the speed of the spray, the distance of the nozzle from the substrate, and the substrate temperature, a fully-covered perovskite film is obtained. The perovskites made by these methods are characterized and used to prepare PVSCs with the n-i-p structure of fluorine-doped tin oxide (FTO)-coated glass/c-TiO_2/$CH_3NH_3PbI_3$/spiro-OMeTAD/Au, where spiro-OMeTAD is the short form for 2,2′,7,7′-Tetrakis[*N*, *N*-di(4-methoxyphenyl)amino]-9,9′-spirobifluorene, and c-TiO_2 is a compact layer of TiO_2. Figure 1 shows the schematic diagram of the casting methods used in this work to fabricate the perovskite layer in a two-step sequential process.

2 Experimental Details

2.1 *Materials and Methods*

Lead iodide (PbI_2, 98.5%), *N*, *N*-dimethylformamide (DMF, 99.8%), hydrogen chloride (HCl, 37.5%), ethanol (99.9%), toluene (98.8%) and titanium (IV) isopropoxide (97%), spiro-OMeTAD, 4-tert-butylpyridine (96%), acetonitrile (99.8%), and bis(tri-fluoromethane)sulfonamide lithium salt (99.95%) were purchased from Sigma-Aldrich. Methylammonium iodide (MAI, 99.5%) was purchased from Xi'an Polymer Light Technology Co, China.

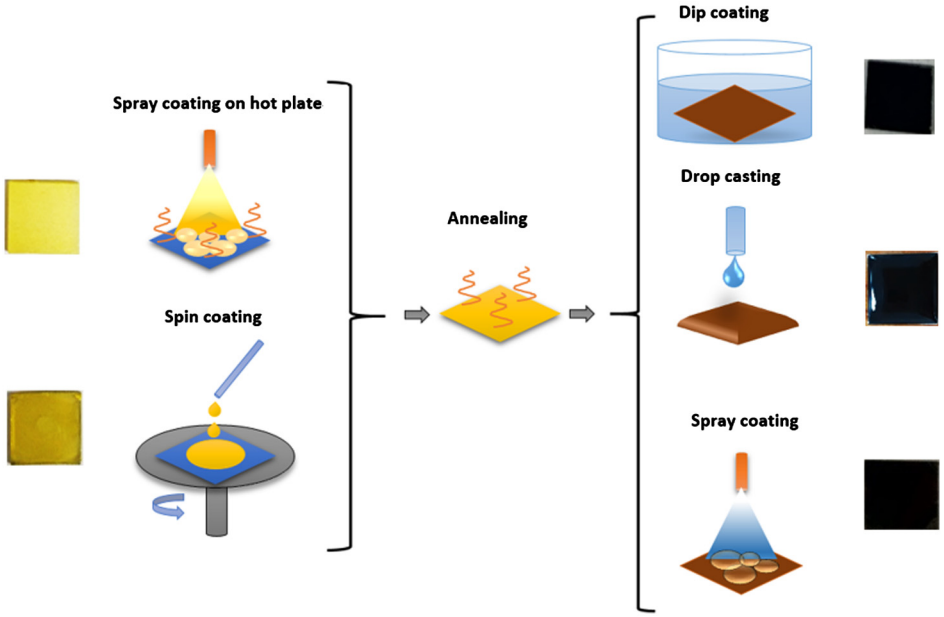

Fig. 1 Schematic diagram of the casting processes used to fabricate perovskite thin films using two-step sequential method. The annealing process of the fabricated perovskite film is not shown.

For optimization and characterization purposes, 10 mm × 10 mm FTO-coated glass substrates were used, whereas for device fabrication, 25 mm × 25 mm substrates were used and etched by zinc powder and HCl solution to achieve a desired pattern. The substrates were washed in deionized water and soap solution, acetone, and isopropyl alcohol by sonication, and then treated in UV–ozone cleaner for 20 min. The c-TiO_2 electron transporting layer was fabricated by spinning the TiO_2 precursor solution on FTO-coated glass at 2000 rpm for 60 s, followed by annealing at 500°C for 1 h. To prepare the TiO_2 precursor solution, 32.5 μl of HCl (2M) was diluted in 2 ml of ethanol and then this solution was added to titanium isopropoxide solution dropwise under stirring condition. Titanium isopropoxide solution was prepared by dilution of 350 μl of titanium isopropoxide in 5 ml of ethanol. The perovskite layer ($CH_3NH_3PbI_3$) was formed atop the c-TiO_2 layer in a two-step sequential process. First, the PbI_2 film was fabricated through spray coating, as well as spin coating, as the reference method. For the spun-on films, PbI_2 was dissolved in DMF in four molarities of 0.2, 0.5, 0.7, and 1 M, and the solution was spun at 2000 rpm for 30 s. Then the film was annealed at 90°C for 30 min. The spray-on PbI_2 films were fabricated using 0.7 M solution of PbI_2 (323 mg of PbI_2 dissolved in 1 ml of DMF). Before use, the solutions were heated at 60°C for 1 h and then cooled at room temperature. Spray coating of PbI_2 film was conducted using a spray-coating machine (Holmarc Opto-Mechatronics Pvt. Ltd., Model HO-TH-04, Kerala, India) in air, using air-assist spray nozzle. The flow rate was kept constant at 1000 μl/ min and the spray nozzle atomization air pressure was tuned at 2 bars. Other spray parameters including the height (nozzle–substrate distance), the speed of the nozzle movement over the substrate (or speed of substrate movement with respect to a stationary nozzle), the number of spray passes, and temperature of the substrate were varied to find the optimum values for the best PbI_2 film characteristics. To mimic the real situation in PVSC fabrication, for the optimization process, all PbI_2 films were deposited onto FTO-coated glass/c-TiO_2. During spray coating of PbI_2, the substrate temperature was set at specific values. Finally, all PbI_2 samples were transferred to an oven for annealing at 90°C for 30 min.

In the second step, dip coating, spray coating, and drop casting were used to deposit the MAI solution. In dip-coating experiments, some spun-on and spray-on PbI_2 samples were dipped in 2 ml of MAI solution, for 5, 20, or 60 min (MAI was dissolved in 2-propanol to obtain concentration of 10 mg/ml). In drop casting experiments, 30 μl of the MAI solution was dripped on PbI_2 films from 2 cm above the film each time. This process was repeated every 5 min to obtain various samples for further analysis. In the experiments where spray coating was used as the method for deposition of the MAI solution, a small spray gun placed in the glovebox was used.

This was done because spray coating of MAI in air resulted in decomposition of perovskite. The spray gun was kept at an optimum distance of 5 cm from the PbI_2 samples. A total of 2 ml of the MAI solution was deposited by pulsed-spray coating for 20 min, in time intervals of 1 min to allow sufficient time for solvent evaporation. In each pulse, 100 μl of MAI solution was sprayed on the PbI_2 film within 1 s, which wetted the PbI_2 film completely. All perovskite samples made using various methods were put on a hotplate in the glovebox and annealed at 90°C, for 2 h.

Spiro-OMeTAD solution was prepared by mixing 60 mg of spiro-OMeTAD, 480 mg/mL of the lithium salt in acetonitrile, and 20 μl of 4-tert-butyloyridine. The solution was deposited atop the perovskite layer through spin coating in the glovebox at 2000 rpm for 30 s, and the samples were kept there for 12 h. To complete the device, 100 nm of gold was thermally evaporated atop the spiro-OMeTAD film. The devices were encapsulated using glass and UV-treated epoxy. The samples were partially exposed to high ambient humidity (50% to 70%) during transfer from the glovebox to the thermal evaporator as well as during the device encapsulation.

2.2 *Film and Device Characterization*

Optical microscopy images of PbI_2 films were taken by a confocal laser scanning microscope (CLSM 700, ZEISS, Oberkochen, Germany) at magnification of 20× (700 μm × 525 μm) and 50× (275 μm × 210 μm), while scanning electron microscopy (SEM, Hitachi, Model S-3400N, Japan) was used to study the surface topography of perovskite films. Optical images with magnification of 20× were imported to ImageJ software to analyze and estimate the coverage of PbI_2 and perovskite films. Film thickness and profile roughness (Ra: arithmetic average of peaks and valleys) were measured using a stylus profiler (KLA-Tencor P7). To measure the roughness, random lines with a length of at least 1 mm were selected on the surface of each sample. The film thickness was measured with respect to the cleaned edges of the samples. Coverage, roughness, and thickness experiments were run in triplicate. X-ray diffraction (XRD, model D5005, Bruker, Germany) analysis was performed to study the crystal structure of the perovskite films. UV-visible absorbance spectra of perovskite films were obtained using UV-vis spectrophotometer (EV300, Thermo Fisher Scientific, Waltham, Massachusetts). Photoluminescence (PL) characterization was performed using PTI-QM/TM/IM PL spectrometer with PL-F2X nitrogen laser as the excitation source. The PV parameters of the fabricated devices ($J-V$ curves) were measured by a Keysight source meter Model B2902A, Japan, in the forward direction with normal mode scan speed and under AM1.5G solar irradiation with an intensity of 100 mW cm^{-2}. Before the test, the light intensity was calibrated using a standard Si SC.

3 Results and Discussion

3.1 *PbI_2 Films*

The first step in two-step sequential fabrication of a perovskite layer is to prepare a uniform PbI_2 film with high coverage to work as a template for the formation of perovskite crystals. As the first step, the concentration of PbI_2 solution was optimized. Figures 2(a)–2(d) show optical images of spun-on PbI_2 films, prepared at various concentrations, and SEM images of their corresponding perovskite films, made by spin-dip coating. Figure 3 shows the thickness and roughness of the PbI_2 films and quantitative values of the coverage of PbI_2 and perovskite films prepared at various concentrations of the PbI_2 solution. Figure 2 shows that large PbI_2 crystals form at a concentration of 1 M. Although this concentration has been frequently applied in mesoporous structures,[9,38] it is found that this concentration is not suitable for planar structures. On the other hand, the uniform and fully covered spun-on PbI_2 film prepared using 0.2 M solution shows excessive voids in the corresponding perovskite film, due to the lack of sufficient PbI_2. Therefore, the PbI_2 solution concentrations of 0.5 and 0.7 M are desirable, albeit at 0.5 M, the corresponding perovskite film shows a lower coverage than that of the 0.7 M. Figure 3 shows that as the concentration of PbI_2 solution increases, the roughness and thickness of the PbI_2 film increases almost linearly. The coverage of the PbI_2 film decreases as the PbI_2 solution concentration increases, because larger PbI_2 crystals form at a higher concentration, resulting in crystallization dewetting.[13] It appears that the coverage of perovskite films depends

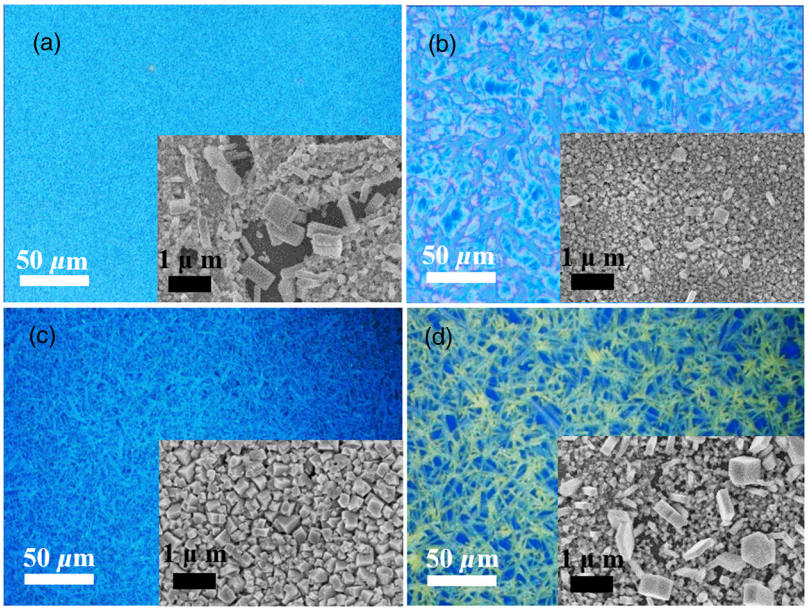

Fig. 2 Optical images of spun-on PbI_2 films fabricated at various solution concentrations. (a) 0.2, (b) 0.5, (c) 0.7, and (d) 1 M solution. The SEM inset images show the corresponding spin-dip perovskite films.

on high or adequate coverage of the PbI_2 film (achieved at PbI_2 concentration of 0.5 and 0.7 M), and the presence of sufficient PbI_2 for a satisfactory conversion of precursors into perovskite. In agreement with this argument, Fig. 3(c) shows that the highest coverage of perovskite is obtained at PbI_2 solution concentration of 0.7 M. It is noted that with a change in spin-coating conditions and thus the PbI_2 film thickness, the optimum concentration may change.

Having found the optimum concentration of PbI_2 solution for the highest coverage of spun-on PbI_2 (~0.5 to 0.7 M) and spin-dip perovskite films (~0.7 M), spin coating was then replaced by spray coating. Our preliminary experiments showed that the application of multiple spray passes while the substrate is kept at ambient temperature may have a disruptive effect on the morphology of the entire film, because the forthcoming spray passes may disturb the existing wet film. To support this argument, Fig. 4 shows the effect of the number of spray passes (1 and 3 passes) on the morphology of the perovskite films, prepared after dipping the spray-on PbI_2 films into the MAI solution, where the spray nozzle height and speed were kept at 10 cm and 50 mm/s, respectively, the substrate temperature was kept at ambient temperature of 25°C, and the PbI_2 solution concentration was set to 0.5 M. At room temperature, increasing the number of spray passes from 1 to 3 results in an increase in the PbI_2 film roughness and thickness that may

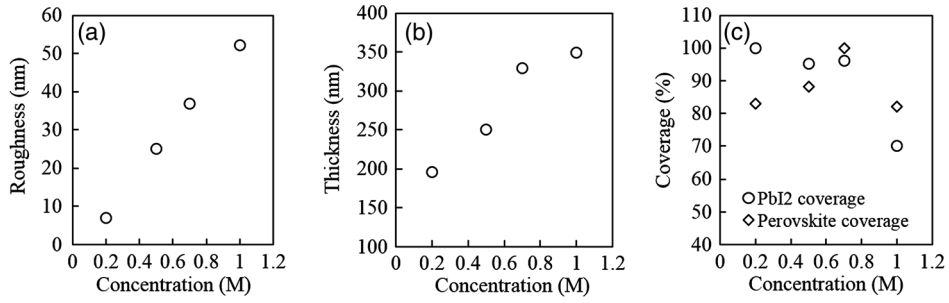

Fig. 3 Variation of (a) roughness and (b) thickness of spun-on PbI_2 films against PbI_2 in DMF solution concentration, and (c) coverage of spun-on PbI_2 films and their corresponding spin-dip perovskite films versus concentration of PbI_2 solution. The PbI_2 solutions were spun at 2000 rpm, for 30 s.

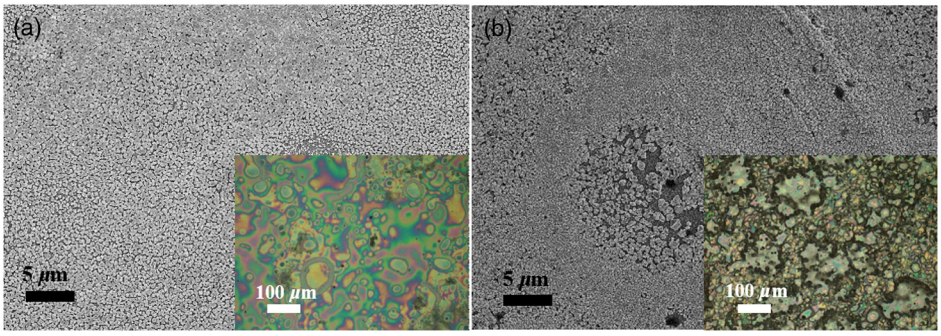

Fig. 4 SEM images of perovskite films and optical images of their corresponding PbI_2 films (inset), using (a) one spray pass and (b) three spray passes. PbI_2 concentration = 0.5 M; spray nozzle height = 10 cm; spray nozzle speed = 50 mm/s; substrate temperature = 25°C; and dipping time = 1 h.

cause low conversion of PbI_2 to perovskite, because a high thickness hampers penetration of the MAI solution into the lower parts of the PbI_2 film. This hypothesis is backed by the XRD patterns of Fig. 5, showing the peaks of the perovskite made using the spray-dip method, at one and multiple spray passes (spray height = 10 cm; nozzle speed = 50 mm/s; and substrate temperature = 25°C). The first peak observed in the film made using four passes, around 12 deg, belongs to PbI_2, which is not observed in the pattern of fully converted perovskite film made using one pass. The peaks near 14.2 deg and 28.6 deg in both graphs are associated with the perovskite structure.

Although the PbI_2 film prepared using one pass shows a high coverage at the first glance (c.f. Fig. 4), pinholes due to partial crystallization dewetting are observed in the film. Figures 2 and 3 had shown that a PbI_2 concentration of ~0.5 to 0.7 M is favorable. Therefore, in another series of experiments, the concentration of PbI_2 film was set to 0.7 M, while spray speed and height of the nozzle were tuned to optimum values to avoid the formation of thick wet films. For the spray nozzle and flow rate used in this study, we found that the optimum spray height is in the range of 12 to 14 cm, and the optimum spray nozzle speed is about 60 mm/s. For other sprays, a similar procedure may be followed to arrive at similar conclusions.[39] It is found that in ambient temperature, a prolonged drying time may lead to dewetting of the liquid film due to growth of the hydrodynamic perturbations, as well as crystallization dewetting during solvent evaporation.[13] To overcome this problem, the substrate temperature may be increased to decrease the film drying time to cure and solidify the film before the perturbations grow and destabilize the thin liquid film. Elevated temperature and rapid solidification may control the crystallization dewetting as well by arresting excessive growth of the crystals.

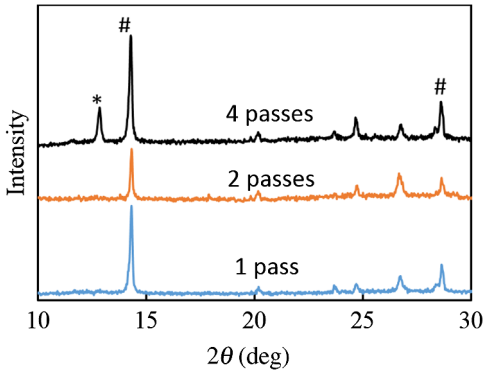

Fig. 5 Effect of the number of spray passes on perovskite conversion. XRD patterns of perovskite films prepared using spray-dip coating, showing high conversion (one spray pass) and incomplete conversion (four passes). * represents PbI_2 and # represents perovskite peaks. PbI_2 concentration = 0.7 M; spray nozzle height = 10 cm; spray nozzle speed = 50 mm/s; substrate temperature = 25°C; and dipping time = 1 h.

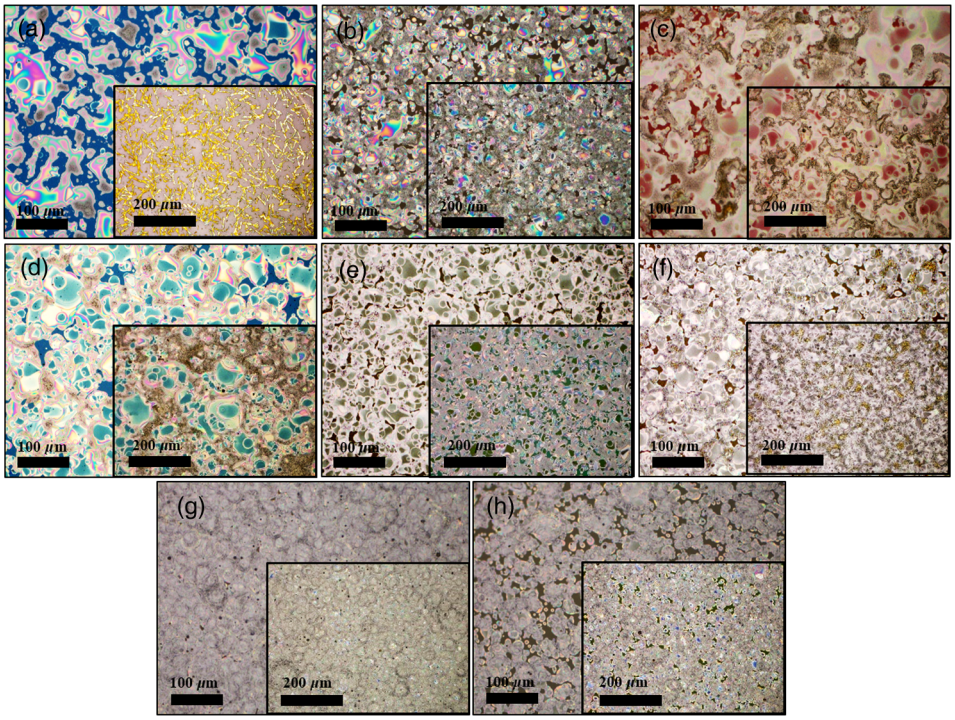

Fig. 6 Optical images of spray-on PbI_2 films fabricated using one spray pass (main images) and two spray passes (inset) at substrate temperatures of (a) 25°C, (b) 40°C, (c) 50°C, (d) 60°C, (e) 75°C, (f) 100°C, (g) 160°C, and (h) 200°C. PbI_2 solution concentration = 0.7 M; spray nozzle height = 12 cm; and spray nozzle speed = 60 mm/s.

Following the aforementioned argument on the effect of the substrate temperature, the substrates were heated to several temperatures below the boiling point of DMF (153°C), including 40°C, 50°C, 60°C, 75°C, and 100°C, and a temperature near the boiling point of DMF, i.e., 160°C and a temperature higher than the boiling point of DMF, i.e., 200°C. Figure 6 shows the optical images of spray-on PbI_2 films, made at the aforementioned temperatures using one and two spray passes, while other parameters are kept constant at the optimum conditions (i.e., spray nozzle height and speed of 12 cm and 60 mm/s, respectively). Figure 7 shows the effect of the substrate temperature on the estimated percentage of the coverage of spray-on PbI_2 films. Figures 6 and 7 collectively show that the coverage of spray-on PbI_2 films increases with the substrate temperature and declines again at temperatures higher than the solvent boiling point and close to the Leidenfrost temperature. One observation is that at low substrate temperature (25°C), a second spray pass severely deteriorates the film coverage, whereas at elevated

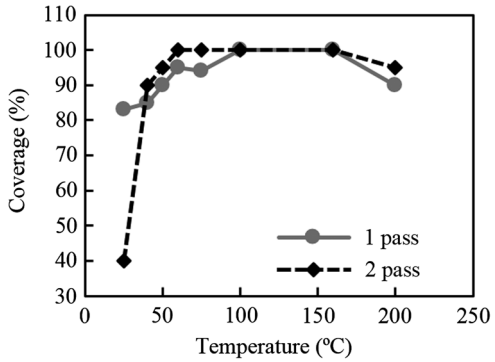

Fig. 7 Effect of substrate temperature on the estimated coverage of spray-on PbI_2 films, fabricated using one and two spray passes. PbI_2 concentration = 0.7 M; spray nozzle height = 12 cm; and spray nozzle speed = 60 mm/s.

temperatures, generally, the application of a second spray pass results in a slightly higher or comparable coverage. These findings are interpreted as follows. In spray coating, impinged droplets spread, making liquid disks or lamellae. At ambient temperature, merging or coalescence of some of these disks that are in close proximity to one another may form a wet film or several patches or islands. If the spray flow rate is sufficiently high and droplets impact the substrate rather uniformly, a complete wet film may form through merging of the aforementioned liquid islands. If the flow rate is lower than that required to form a wet film, increasing the number of spray passes delivers more liquid to the substrate, but at the same time disturbs the film. Additionally, in our previous study,[13] we demonstrated that large crystals of PbI_2 may form due to the crystallization dewetting. Therefore, a second pass at low substrate temperature may further contribute to the formation of larger crystals and crystallization dewetting. This is clearly observed in images of Fig. 6(a) and also Fig. 7 for the substrate temperature of 25°C. At elevated temperatures, the impinged solution droplets may dry before complete spreading and coalescence with adjacent droplets, preventing the formation of a wet film. The elevated temperature and rapid solvent evaporation also stop excessive crystal growth and the extent of crystallization dewetting. In summary, at elevated temperatures, the second spray pass helps in filling the dewetted areas of the first pass, whereas at room temperature, the second pass disturbs the wet film of the first pass and deteriorates the film coverage. As the substrate temperature approaches the boiling point of DMF (153°C), the film becomes more continuous. Figures 6 and 7 show that the best coverage occurs using one spray pass at temperatures of 100°C and 160°C, in which the impinged droplets dry after adequate spreading. As the temperature increases further (200°C), the coverage is deteriorated because of insufficient spreading. Moreover, the solvent may partially evaporate before impingement causing a decrease in droplet size.[39] Also, at high substrate temperatures, close to the solvent Leidenfrost temperature, rapid evaporation of solvent upon impact and the formation of a vapor layer may cause droplet deflection, which disturbs droplet spreading resulting in a low coverage.[40]

Figure 8 displays the XRD patterns and SEM images of perovskite films made using two-step sequential spray-dip coating. The PbI_2 at concentration of 0.7 M was sprayed using one pass at optimum conditions. In spite of obtaining the highest coverage at substrate temperatures of 100°C and 160°C using one spray pass (Figs. 5 and 6), the XRD patterns of the resulting perovskite films shown in Fig. 8 clearly illustrate a low conversion of PbI_2 to perovskite, for the cases where PbI_2 was deposited at high substrate temperatures of 75°C and 100°C. In other words, PbI_2 crystals processed at elevated temperatures have not adequately converted to perovskite.

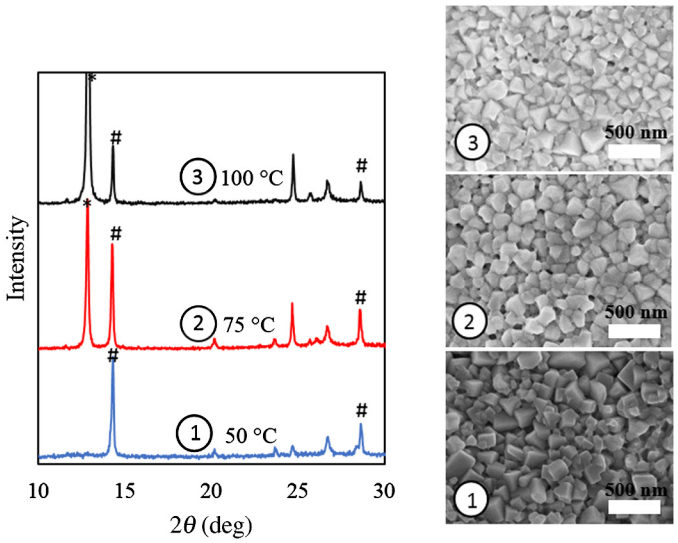

Fig. 8 XRD patterns of spray-dip perovskite films fabricated using spray-on PbI_2 films at substrate temperature of 50, 75, and 100°C, and their corresponding SEM images. * represents PbI_2 and # represents perovskite peaks. PbI_2 concentration = 0.7 M; spray nozzle height = 12 cm; spray nozzle speed = 60 mm/s; and dipping time = 1 h.

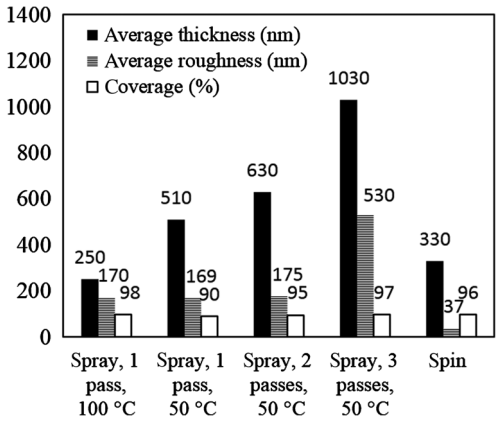

Fig. 9 Thickness, roughness, and coverage of spray-on and spun-on PbI_2 films. PbI_2 concentration = 0.7 M; spray nozzle height = 12 cm; and spray nozzle speed = 60 mm/s.

This may be due to partial sintering and hardening of PbI_2 crystals at elevated temperatures, also resulting in elimination of grain boundaries and crystal interfaces in the PbI_2 film. The hardened PbI_2 crystals with few grain boundaries cannot be easily infiltrated by the MAI solution. Figure 8 shows that full perovskite conversion only occurs at a temperature of 50°C. On the other hand, according to Fig. 7, substrate temperatures lower than 100°C cannot result in a fully covered spray-on PbI_2 film, but increasing the number of spray passes may improve the coverage, provided that the substrate is heated. Thus, overall, the coverage of PbI_2 films sprayed in two passes is better than those deposited using one spray pass. Although the film fabricated using two spray passes at 50°C shows a better coverage (95%) than that with one spray pass (90%) (Fig. 7) and conversion (Fig. 8), its roughness and thickness are higher compared to the film fabricated using one pass (Fig. 9). Therefore, there must be a trade-off between coverage, roughness, and conversion to specify the optimum conditions for the fabrication of spray-on PbI_2 films. The optimum parameters are identified as a substrate temperature of around 50°C, and two spray passes to achieve the best PbI_2 film in terms of coverage, conversion, and uniformity. Figure 9 shows that the perovskite sample made using three spray passes is rough and thick and not favorable. It is noted that the spray flow rate and concentration of PbI_2 solution obviously are important parameters. The spray flow rate should be carefully selected to deliver adequate solution to the film to ideally facilitate the formation of a continuous thin liquid film. As mentioned before, suitable concentration of PbI_2 in DMF and spray flow rate were identified as 0.7 M and 1000 μl/s, respectively.

PL spectra of perovskite films, deposited on c-TiO_2 film by spray-dip coating, are shown in Fig. 10 to demonstrate the importance of coverage in charge collection in PVSCs. Both perovskite films have an emission peak at 773 nm. Lack of full coverage in the sample prepared using one spray pass causes lower extraction of electrons from the perovskite film, which results in a higher PL intensity, in agreement with a similar work[22] on mixed halide perovskites sprayed using the one-step method. It is noted that the two films have different thicknesses, i.e., the high coverage film prepared using two spray passes has a higher thickness compared to the low-coverage film prepared using one spray pass. As shown later in this paper, the absorbance is affected by the fabrication process and, therefore, the thickness. Thus, to be more precise, both coverage and thickness affect the PL, although it is deduced that coverage has the main effect.

3.2 *Spray-on Versus Spun-on PbI_2 Films*

In this section, the characteristics of spray-on PbI_2 films are compared with their lab-scale spun-on counterparts to reveal the merits and potential of spray coating. Figure 9 shows that the thickness of the film made using one spray pass at 100°C is less than that of the spun-on sample, but the thicknesses of the films made using one, two, and three spray passes at 50°C are higher than that of the spun-on film. The roughness values reveal that spray-on films in all the conditions are rougher than spun-on films; nevertheless in all cases the coverage is as high as 90% or higher.

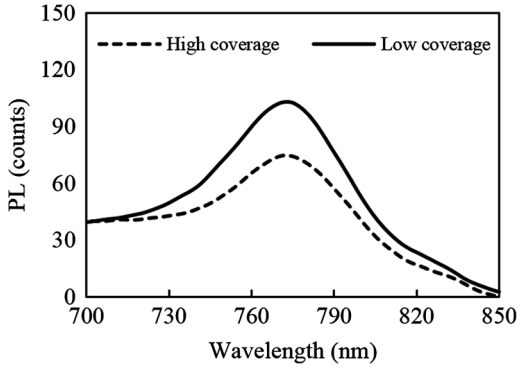

Fig. 10 The effect of the film coverage on the PL spectra of perovskite films made on c-TiO_2 films, using spray-dip coating. The low coverage film (83%) was made using one spray pass on a substrate kept at 25°C, while the high coverage film (95%) was made using two spray passes on a substrate kept at 50°C. PbI_2 concentration = 0.7 M; spray nozzle height = 12 cm; spray nozzle speed = 60 mm/s; and dipping time = 1 h.

Conversion of PbI_2 to perovskite made using spray-dip and spin-dip methods is studied by XRD patterns shown in Fig. 11(a), where a complete conversion is observed in both cases. Additionally, Figs. 11(b) and 11(c) show the optical images of spun-on and spray-on PbI_2 films, and SEM images of the corresponding spin-dip and spray-dip perovskite films, where comparable morphologies are observed, substantiating the merit of spray coating.

3.3 *Perovskite Film*

After achieving optimum conditions for the fabrication of PbI_2 films by spray coating, through investigating the characteristics of the resulting perovskite films made by spray-dip coating, in an attempt to replace the lab-scale dip coating with scalable methods, here we investigate the application of drop casting and spray coating for deposition of the MAI solution atop spun-on

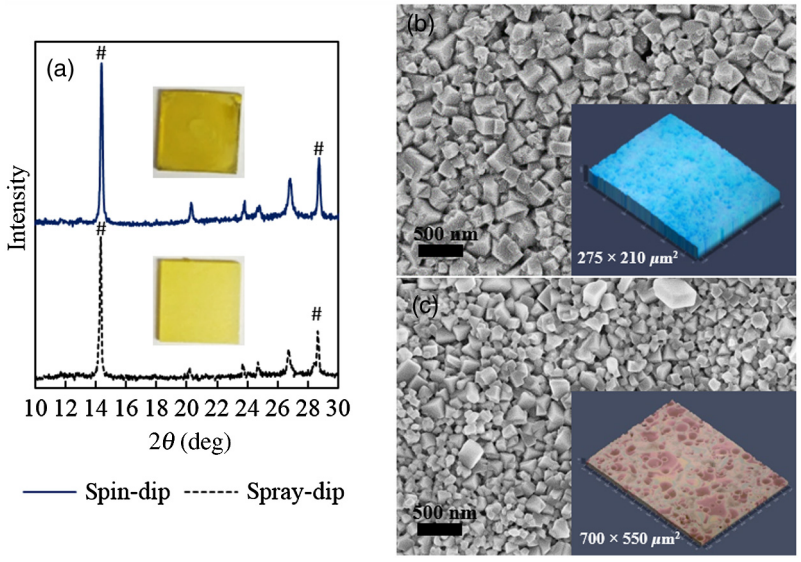

Fig. 11 (a) XRD patterns of spray-dip and spin-dip perovskite films, (b) SEM image of spin-dip perovskite and optical image of the corresponding spun-on PbI_2 film (inset), and (c) SEM image of spray-dip perovskite and optical image of the corresponding spray-on PbI_2 film (inset), prepared using two spray passes. PbI_2 concentration = 0.7 M; substrate temperature = 50°C; spray nozzle height = 12 cm; spray nozzle speed = 60 mm/s; number of spray passes = 2; and dipping time = 1 h. # in XRD patterns represents the perovskite peaks. The height of the films in optical images is not to scale.

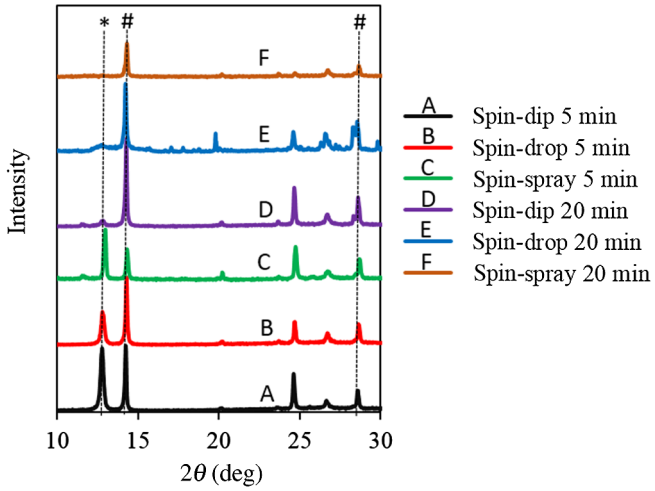

Fig. 12 XRD patterns of perovskite films made by dip coating, drop casting and spray coating of the MAI solution on identical spun-on PbI_2 films. * represents PbI_2 and # represents perovskite peaks. In dip coating method, spun-on PbI_2 films were dipped into 2 ml of MAI solution for a specific time. In drop casting, every 5 min, 30 μl of MAI solution was dripped atop the PbI_2 film. To apply pulsed-spray on spun-on PbI_2 films, 100 μl of MAI solution was sprayed onto the PbI_2 film for 1 s. This process was repeated for 5 and 20 min with time steps of 1 min.

PbI_2 films. In dip coating, 2 ml of MAI solution was consumed to convert spun-on PbI_2 film to perovskite. In drop casting, 30 μl of MAI was dripped on each PbI_2 sample in 5 min time intervals until full conversion was achieved. The XRD patterns in Fig. 12 show that full conversion of PbI_2 to perovskite is achieved after 20 min in all three techniques by appearance of peaks at 14.2 deg and 28.6 deg, which correspond to (110) and (220) planes of perovskite structure. To spray the MAI solution atop the spun-on PbI_2 films, a pulsed-spray technique was used to allow for solvent evaporation during multiple pulses. For this purpose, 100 μl of MAI solution was sprayed in 1 s. This process was repeated for 20 times in intervals of 1 min to achieve a full conversion, consuming 2 ml of the MAI solution. Therefore, in drop casting, only $120(=4\times30)$ μl of MAI solution was used compared to 2 ml of MAI solution used in dip coating and spray coating. Therefore, drop casting significantly reduces wastage of the MAI solution, given that in dip coating, the concentration and purity of the MAI solution will be altered when it is used once, and therefore cannot be reused.

The absorbances of various perovskite films are shown in Fig. 13. In Fig. 13(a), the PbI_2 layer was deposited by spin coating, whereas in Fig. 13(b) spray coating (two spray passes, at the

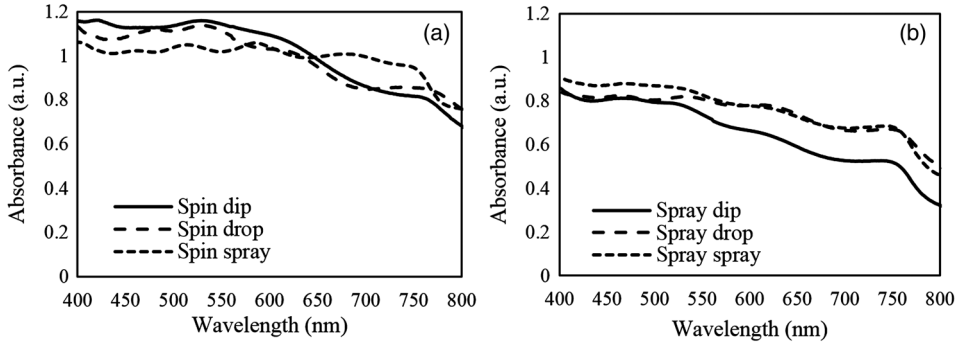

Fig. 13 The absorbance spectra of perovskite films fabricated by (a) spin coating and (b) spray coating, as the deposition method for the PbI_2 layer. The MAI solution was deposited using dip, drop, and spray coating. Spray coating of PbI_2 solution was performed based on two spray passes. Spray coating of the MAI solution was performed using pulsed-spray coating, as outlined in the text. PbI_2 concentration = 0.7 M; substrate temperature = 50°C; spray nozzle height = 12 cm; spray nozzle speed = 60 mm/s; and dipping time = 1 h.

substrate temperature of 50°C) was used to deposit the PbI_2 layer. The MAI solution was deposited by drop, dip, and pulsed-spray coating. It is observed that when spin coating is used to deposit the PbI_2 layer, a higher absorbance is achieved. Although the perovskite films prepared using spray-on PbI_2 films are thicker than the spun-on counterparts (c.f. Fig. 9), Fig. 13 shows that the absorbance of the former is lower than the latter. This may be attributed to the high roughness in spray-on films[10] (c.f. Fig. 9). An important result of Fig. 13 is the comparable absorbance of the films made by drop casting, dip coating, and pulsed-spray coating of MAI solution atop PbI_2.

3.4 *Device Performance*

In the last step, PVSCs were fabricated using spin-drop and spray-drop methods, using optimum PbI_2 solution concentration of 0.7 M. Spin coating (reference method) and spray coating (scalable) were used to fabricate the PbI_2 layer. For deposition of the MAI solution, drop casting was chosen owing to its low solution consumption and comparable performance with respect to dip and pulsed-spray coating. For spray coating, two pass spray coatings at a substrate temperature of 50°C, a spray nozzle height of 12 cm, and spray nozzle speed of 60 mm/s were used. Figures 14(a) and 14(b) show the SEM cross-sectional images of the representative fabricated devices, without the back contact. The images show that a thin and uniform layer of spun-on c-TiO_2 with a thickness of less than 100 nm has formed. The perovskite film prepared using spray-drop coating is thicker and less uniform compared to that made using spin-drop coating. The current density–voltage characteristics and a summary of their PV performance parameters are shown in Fig. 14(c) and Table 1, respectively. The inset image in Fig. 14(c) is a picture of an array of spray-drop devices fabricated on one substrate, where the area of each cell is 9 mm^2. The highest performance was obtained from a spin-drop cell with the short circuit current J_{sc} of 15.9 mA/cm^2, open circuit voltage (V_{oc}) of 0.94 V, FF of 0.634, and PCE of 9.48%, whereas the PCE of the best spray-drop cell is 6.92%, corresponding to J_{sc} of 15.6 mA/cm^2, V_{oc} of 0.88 V, and FF of 0.504. The average PCE obtained from spin-drop cells (8.45%) is also higher than the average value of spray-drop cells (5.95%). The modest device PCE is partly attributed to the exposure of the samples to the high humidity of Shanghai, China, before and after thermal evaporation and during encapsulation. Nevertheless, the results are adequate because the objective of this work is to develop and test facile spray coating and drop casting techniques and to compare the results with those obtained from reference devices fabricated at similar conditions. As mentioned before, the high roughness in the spray-drop perovskite results in a decrease in

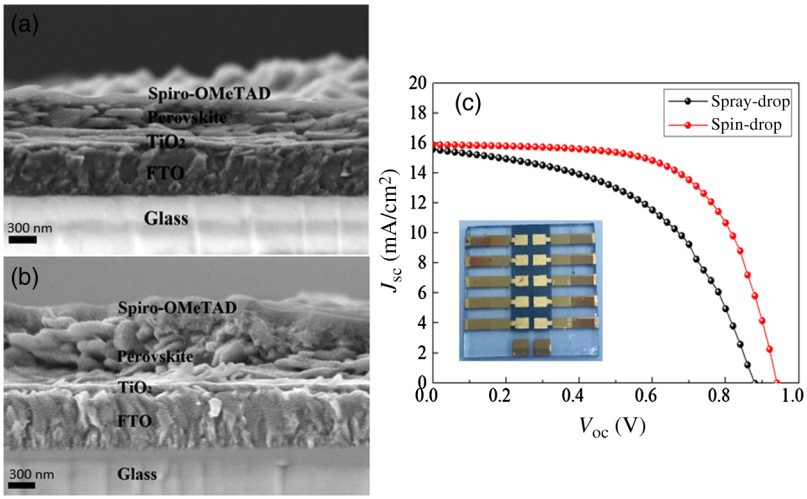

Fig. 14 SEM cross-sectional images of planar PVSCs without the back contact, fabricated by (a) spin-drop and (b) spray-drop coating. (c) $J-V$ curves of PVSCs, where the perovskite layer is fabricated by spin-drop and spray-drop coating. The inset image is the picture of the devices made by spray-drop technique.

Table 1 Photovoltaic performance of the PVSCs fabricated using spin-drop and spray-drop methods.

Method		V_{oc} (V)	J_{sc} (mA/cm^2)	FF (%)	PCE (%)
Spin-drop	Best device	0.94	15.9	63.4	9.48
	Average	0.92	15.83	57.78	8.45
Spray-drop	Best device	0.88	15.6	50.4	6.92
	Average	0.87	15.53	43.72	5.95

the absorbance[10] and the FF,[34] where the latter is due to the increased contact resistance between the nonuniform spray-on layer and its adjacent layers. Also, presumably larger numbers of pinholes in spray-drop perovskite compared to spin-dip device cause a decrease in the shunt resistance creating paths for recombination.[37] The V_{oc} of the spin-drop device is ~0.05 V higher than that of the spray-drop device. This may be explained as follows. The relatively nonuniform perovskite film made by spray coating may increase the population of pinholes, raising the probability of recombination due to detrimental connection between the electron and hole transporting layers, leading to a decrease in V_{oc}. The smoother and more uniform surface of spin-drop perovskite films results in a decrease in pinholes and voids in the interfaces of the active layer with the upper and lower layers, leading to a lower recombination at the interfaces and a higher V_{oc}.[37] Lower current density of the spray-drop device may stem from the lower absorbance of spray-drop perovskite films compared to the spin-drop films (c.f. Fig. 13). In addition to lower absorbance, higher recombination in spray-drop perovskite films compared to spin-drop films may cause a lower J_{sc}. Overall, the difference between the average value of the PCE of the spray-drop and spin-drop devices is about 2.5%, which may be considered acceptable for the spray-drop devices, fabricated using scalable and touch-free coating techniques. It is noted that for commercialization purposes, it is desirable to fabricate all layers using the same scalable method, such as spray coating, but this work focused on the optimization process of the perovskite layer only and the electron- and hole-transporting layers were prepared by conventional spin coating. As to the other layers, as long as the material is solution-processed, it could be deposited using scalable methods, such as spray and blade coating, although fabrication of very thin layers may be challenging. The c-TiO_2 layer could be readily deposited by spray pyrolysis[41] and research is currently being undertaken to substitute flexible spray-on graphene-based[42] and nanowire-based[43] electrodes for the current (front and back) electrodes, in an attempt to achieve fully solution processed and transparent conducting oxide-free devices.

4 Conclusion

This study focused on optimization of the spray-coating parameters to achieve a fully covered spray-on PbI_2 film as the first step in a sequential deposition of methylammonium lead iodide perovskite layer. Then in the second step, the MAI solution was deposited atop the spray-on and spun-on PbI_2 films by pulsed-spray and also by drop casting as two facile and scalable techniques as well as by conventional dip-coating technique. The optimum concentration of PbI_2 in DMF was found to be ~0.5 to 0.7 M within the experimental conditions of this work. Then, for the spray nozzle used in the work, the spraying conditions were optimized systematically, where the approach can be generalized to other sprays. The optimum number of spray passes varies with the substrate temperature. If the substrate is kept at room temperature, the application of additional spray passes may deteriorate the coverage, whereas at elevated substrate temperatures, where the impinged spray droplets dry rather quickly, application of additional passes improves the coverage. Using multiple spray passes also increases the roughness and thickness of the PbI_2 film, thus reducing the chance of PbI_2 conversion to perovskite, due to higher film thicknesses. As the substrate temperature increases and approaches the boiling point of the PbI_2 solvent, viz. DMF (153°C), the best coverage occurs, even using one spray pass. However, we observed that at elevated substrate temperatures, due to partial sintering and hardening of the PbI_2 crystals, the

MAI solution cannot infiltrate the hardened PbI_2 film, thus a full conversion of MAI and PbI_2 precursors to perovskite was not observed. Consequently, for the nozzle and flow rate used in this study, based on a trade-off between coverage, roughness, thickness, and full conversion, the optimum substrate temperature in a sequential deposition is identified to be around 50°C using two spray passes.

Subsequently, drop casting and pulsed-spray coating, as well as dip coating, were applied on spun-on films (as the reference samples) and also on spray-on PbI_2 films, to make perovskite films, where the samples fabricated through the three foregoing techniques on spray-on PbI_2 films showed lower absorbance compared to their counterparts fabricated on spun-on PbI_2 films, due to the higher roughness of spray-on PbI_2 films. However, the three techniques used in the second step for deposition of the MAI solution led to the comparable absorbance, both on spun-on and spray-on PbI_2 films. Moreover, it was shown that the consumption of the MAI solution in drop casting is much less than those in dip and spray coating. Finally, devices were fabricated using spin-drop and spray-drop methods, where the best spin-drop device showed higher PCE of 9.48% compared to 6.92% for the best spray-drop device. The results reveal the capability of spray coating and drop casting for the low-cost fabrication of perovskite SCs.

Acknowledgments

Research funding from the Shanghai Municipal Education Commission in the framework of oriental scholar and funding from the National Natural Science Foundation of China (NSFC) is acknowledged.

References

1. Q. Wang et al., "Progress in emerging solution-processed thin film solar cells—Part I: polymer solar cells," *Renewable Sustainable Energy Rev.* **56**, 347–361 (2016).
2. M. Habibi et al., "Progress in emerging solution-processed thin film solar cells—Part II: perovskite solar cells," *Renewable Sustainable Energy Rev.* **62**, 1012–1031 (2016).
3. National Renewable Energy Laboratory, "Research cell record efficiency chart," 2017, https://www.nrel.gov/pv/assets/images/efficiency-chart.png (December 2016).
4. J. Burschka et al., "Sequential deposition as a route to high-performance perovskite-sensitized solar cells," *Nat. Photonics* **499**, 316–319 (2013).
5. F. Zabihi, M.-R. Ahmadian-Yazdi, and M. Eslamian, "Fundamental study on the fabrication of inverted planar perovskite solar cells using two-step sequential substrate vibration-assisted spray coating (2S-SVASC)," *Nanoscale Res. Lett.* **11**, 71 (2016).
6. C. Huang et al., "Highly efficient perovskite solar cells with precursor composition-dependent morphology," *Sol. Energy Mater. Sol. Cells* **145**, 231–237 (2016).
7. C. C. Chen et al., "One-step, low-temperature deposited perovskite solar cell utilizing small molecule additive," *J. Photonics Energy* **5**, 057405 (2015).
8. M. Liu, M. B. Johnston, and H. J. Snaith, "Efficient planar heterojunction perovskite solar cells by vapour deposition," *Nature* **501**, 395–398 (2013).
9. J. H. Im et al., "Growth of $CH_3NH_3PbI_3$ cuboids with controlled size for high-efficiency perovskite solar cells," *Nat. Nanotechnol.* **9**, 927–932 (2014).
10. L. Wengeler et al., "Comparison of large scale coating techniques for organic and hybrid films in polymer based solar cells," *Chem. Eng. Process. Process Intensif.* **68**, 38–44 (2013).
11. M. Habibi et al., "Defect-free large-area (25 cm^2) light absorbing perovskite thin films made by spray coating," *Coatings* **7**, 42 (2017).
12. M. Eslamian and F. Zabihi, "Ultrasonic substrate vibration-assisted drop casting (SVADC) for the fabrication of photovoltaic solar cell arrays and thin-film devices," *Nanoscale Res. Lett.* **10**, 462 (2015).
13. M. Habibi, A. Rahimzadeh, and M. Eslamian, "On dewetting of thin films due to crystallization (crystallization dewetting)," *Eur. Phys. J. E.* **39**, 30 (2016).
14. M. Hçsel, H. F. Dam, and F. C. Krebs, "Development of lab-to-fab production equipment across several length scales for printed energy technologies, including solar cells," *Energy Technol.* **3**, 293–304 (2015).

15. J. H. Lee, S. Yoshikawa, and T. Sagawa, "Fabrication of efficient organic and hybrid solar cells by fine channel mist spray coating," *Sol. Energy Mater. Sol. Cells* **127**, 111–121 (2014).
16. Y. J. Kang et al., "Progress towards fully spray-coated semitransparent inverted organic solar cells with a silver nanowire electrode," *Org. Electron.* **15**, 2173–2177 (2014).
17. J. G. Tait et al., "Spray coated high-conductivity PEDOT:PSS transparent electrodes for stretchable and mechanically-robust organic solar cells," *Sol. Energy Mater. Sol. Cells* **110**, 98–106 (2013).
18. M. Eslamian and J. Newton, "Spray-on PEDOT:PSS and P3HT:PCBM thin films for polymer solar cells," *Coatings* **4**, 85–97 (2014).
19. Y. Xie, S. Gao, and M. Eslamian, "Fundamental study on the effect of spray parameters on characteristics of P3HT:PCBM active layers made by spray coating," *Coatings* **5**, 488–510 (2015).
20. Y. J. Noh et al., "Cost-effective ITO-free organic solar cells with silver nanowire-PEDOT: PSS composite electrodes via a one-step spray deposition method," *Sol. Energy Mater. Sol. Cells* **120**, 226–230 (2014).
21. A. T. Barrows et al., "Efficient planar heterojunction mixed-halide perovskite solar cells deposited via spray-deposition," *Energy Environ. Sci.* **7**, 2944–2950 (2014).
22. B. A. Nejand et al., "New scalable cold-roll pressing for post-treatment of perovskite microstructure in perovskite solar cells," *J. Phys. Chem. C* **120**, 2520–2528 (2016).
23. S. Das et al., "High-performance flexible perovskite solar cells by using a combination of ultrasonic spray-coating and low thermal budget photonic curing," *ACS Photonics* **2**, 680–686 (2015).
24. J. G. Tait et al., "Rapid composition screening for perovskite photovoltaics via concurrently pumped ultrasonic spray coating," *J. Mater. Chem. A* **4**, 3792–3797 (2016).
25. Y. S. Jung et al., "Differentially pumped spray deposition as a rapid screening tool for organic and perovskite solar cells," *Sci. Rep.* **6**, 20357 (2016).
26. P. S. Chandrasekhar et al., "Fabrication of perovskite films using an electrostatic assisted spray technique: the effect of the electric field on morphology, crystallinity and solar cell performance," *Nanoscale* **8**, 6792–6800 (2016).
27. Z. Liang, X. Xu, and J. Wang, "A facile spray deposition route for uniform perovskite solar cells processed in air international photonics and optoelectronics," in *Int. Photonics and OptoElectronics Conf.*, Optical Society of America, Wuhan (2015).
28. F. Li et al., "A facile spray-assisted fabrication of homogenous flat $CH_3NH_3PbI_3$ films for high performance mesostructure perovskite solar cells," *Mater. Lett.* **157**, 38–41 (2015).
29. Z. Liang et al., "A large grain size perovskite thin film with a dense structure for planar heterojunction solar cells via spray deposition under ambient conditions," *RSC Adv.* **5**, 60562 (2015).
30. N. Mohammadian et al., "A two-step spin-spray deposition processing route for production of halide perovskite solar cell," *Thin Solid Films* **616**, 754–759 (2016).
31. A. K. Chilvery et al., "Efficient planar perovskite solar cell by spray and brush solution-processing methods," *J. Photonics Energy* **5**, 053093 (2015).
32. Z. Bi et al., "Fast preparation of uniform large grain size perovskite thin film in air condition via spray deposition method for high efficient planar solar cells," *Sol. Energy Mater. Sol. Cells* **162**, 13–20 (2017).
33. H. Huang et al., "Two-step ultrasonic spray deposition of $CH_3NH_3PbI_3$ for efficient and large-area perovskite solar cell," *Nano Energy* **27**, 352–358 (2016).
34. C. Girotto et al., "High-performance organic solar cells with spray-coated hole-transport and active layers," *Adv. Funct. Mater.* **21**, 64–72 (2011).
35. G. Susanna et al., "Airbrush spray-coating of polymer bulk-heterojunction solar cells," *Sol. Energy Mater. Sol. Cells* **95**, 1775–1778 (2011).
36. S. Y. Park et al., "Spray-coated organic solar cells with large-area of 12.25 cm^2," *Sol. Energy Mater. Sol. Cells* **95**, 852–855 (2011).
37. M. Ramesh et al., "Using an airbrush pen for layer-by-layer growth of continuous perovskite thin films for hybrid solar cells," *Appl. Mater. Interfaces* **7**, 2359–2366 (2015).

38. C. Sun et al., "Solvent-assisted growth of organic–inorganic hybrid perovskites with enhanced photovoltaic performances," *Sol. Energy Mater. Sol. Cells* **143**, 360–368 (2015).
39. M. Eslamian, "A mathematical model for the design and fabrication of polymer solar cells by spray coating," *Drying Technol.* **31**, 405–413 (2013).
40. M. Eslamian, "Spray-on thin film PV solar cells: advances, potentials and challenges," *Coatings* **4**, 60–84 (2014).
41. T. Supasai et al., "Compact nanostructured TiO_2 deposited by aerosol spray pyrolysis for the hole-blocking layer in a $CH_3NH_3PbI_3$ perovskite solar cell," *Solar Energy* **136**, 515–524 (2016).
42. F. Zabihi and M. Eslamian, "Low-cost transparent graphene electrodes made by ultrasonic substrate vibration-assisted spray coating (SVASC) for thin film devices," *Graphene Technol.* 1–11 (2017).
43. K. Yang et al., "All-solution processed semi-transparent perovskite solar cells with silver nanowires electrode," *Nanotechnology* **27**, 095202 (2016).

Mehran Habibi is a PhD student at the University of Michigan-Shanghai Jiao Tong University Joint Institute and focuses on the fabrication of thin film perovskite solar cells and transistors using scalable methods, such as spray and blade coating.

Mohammad-Reza Ahmadian-Yazdi is an MS degree student at the University of Michigan-Shanghai Jiao Tong University Joint Institute and focuses on the fabrication of perovskite solar cells using ultrasonic vibration-assisted deposition of the perovskite layer for the development of post annealing-free devices.

Morteza Eslamian is an associate professor at the University of Michigan-Shanghai Jiao Tong University Joint Institute and cross appointed at the State Key Lab for Composite Materials, School of Materials Science and Engineering, Shanghai Jiao Tong University. He focuses on thermal fluid sciences and their applications in materials synthesis, such as thin film photovoltaics.